

A tight-binding approach to uniaxial strain in graphene

Vitor M. Pereira and A. H. Castro Neto

Department of Physics, Boston University, 590 Commonwealth Avenue, Boston, MA 02215, USA

N. M. R. Peres

Centro de Física e Departamento de Física, Universidade do Minho, P-4710-057, Braga, Portugal

(Dated: April 21, 2022)

We analyze the effect of tensional strain in the electronic structure of graphene. In the absence of electron-electron interactions, within linear elasticity theory, and a tight-binding approach, we observe that strain can generate a bulk spectral gap. However this gap is critical, requiring threshold deformations in excess of 20%, and only along preferred directions with respect to the underlying lattice. We discuss how strain-induced anisotropy and local deformations can be used as a means to sustain reversible current flow in graphene devices.

PACS numbers: 81.05.Uw, 62.20.-x, 73.90.+f

It is now well established that sp^2 bonded carbon systems feature record-breaking mechanical strength and stiffness. Investigations in the context of carbon nanotubes reveal intrinsic strengths [1] that make these systems the strongest in nature. Recently, graphene — the mother of all sp^2 carbon structures — has been confirmed as the strongest material ever measured [2], being able to sustain reversible deformations in excess of 20% [3].

These mechanical measurements arise at a time where graphene draws considerable attention on account of its unusual and rich electronic properties. Besides the great crystalline quality, high mobility and resilience to high current densities [4], they include a strong field effect [5], absence of backscattering [6] and a minimum metallic conductivity [7]. While many such properties might prove instrumental if graphene is to be used in future technological applications in the ever pressing demand for miniaturization in electronics, the latter is actually a strong deterrent: it hinders the pinching off of the charge flow and the creation of quantum point contacts. In addition, graphene has a gapless spectrum with linearly dispersing, Dirac-like, excitations [8, 9]. Although a gap can be induced by means of quantum confinement in the form of nanoribbons [10] and quantum dots [11], these “paper-cutting” techniques are prone to edge roughness, which has detrimental effects on the electronic properties. Hence, a route to induce a robust, *clean*, bulk spectral gap in graphene is still much in wanting.

In this paper we inquire whether the seemingly independent aspects of mechanical response and electronic properties can be brought together with profit in the context of a tunable electronic structure. Motivated by recent experiments showing that reversible and controlled strain can be produced in graphene with measurable effects [12, 13], we theoretically explore the effect of strain in the electronic structure of graphene within a tight-binding approach. Our calculations show that, in the absence of electron-electron interactions, a gap can be opened in a pure tight binding model of graphene for

deformations beyond 20%. This gap opening is not a consequence of a broken sublattice symmetry but due to level crossing. The magnitude of this effect depends on the direction of applied tension, so that strain along a zig-zag direction is most effective in overcoming the gap threshold, whereas deformations along an armchair direction do not induce a gap.

Model – We take electron dynamics of electrons hopping in the honeycomb lattice as being governed by the nearest neighbor tight-binding Hamiltonian

$$H = \sum_{\mathbf{R}, \boldsymbol{\delta}} t(\mathbf{R}, \boldsymbol{\delta}) a^\dagger(\mathbf{R}) b(\mathbf{R} + \boldsymbol{\delta}) + \text{H. c.} \quad (1)$$

\mathbf{R} denotes a position on the Bravais lattice, and $\boldsymbol{\delta}$ connects the site \mathbf{R} to its neighbors; $a(\mathbf{R})$ and $b(\mathbf{R})$ are the field operators in sublattices A and B. Under general stress conditions, the hopping $t(\mathbf{R}, \boldsymbol{\delta})$ will be generally different among different neighbors. We are interested in the elastic response, for which deformations are affine. This means that even though the hoppings from a given atom to its neighbors can be all different, they will be the same for every atom. Therefore, as depicted in Fig. 1(b), we need only to consider three distinct hoppings: $t_1 = t(\boldsymbol{\delta}_1)$, $t_2 = t(\boldsymbol{\delta}_2)$, and $t_3 = t(\boldsymbol{\delta}_3)$. The relaxed

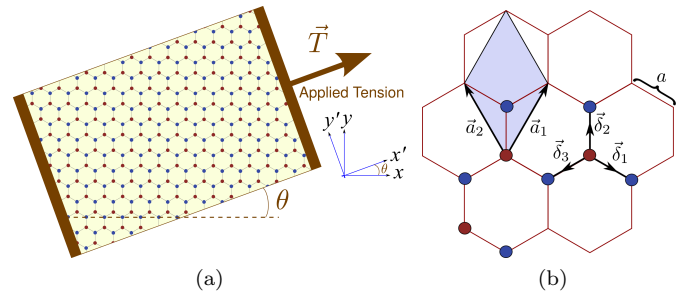


FIG. 1: (Color online) (a) Tension geometry considered in the text. (b) Honeycomb lattice geometry. The vectors $\boldsymbol{\delta}_1 = a(\frac{\sqrt{3}}{2}, -\frac{1}{2})$, $\boldsymbol{\delta}_2 = a(0, 1)$, $\boldsymbol{\delta}_3 = a(-\frac{\sqrt{3}}{2}, -\frac{1}{2})$ connect A-sites to their B-site neighbors.

equilibrium value for $t(\delta_\alpha)$ is $t_0 = t(\delta_\alpha^0) \approx 2.7\text{eV}$ [9]. Our goal is to investigate how strain affects these hoppings, and what impact that brings to the electronic structure (in what follows we use t_0 as the energy unit and the C–C equilibrium distance, $a_0 = 1.42 \text{ \AA}$, as unit of length).

Analysis of Strain – We are interested in uniform planar tension situations, like the one illustrated in Fig. 1(a): the graphene sheet is uniformly stretched (or compressed) along a given direction. The Cartesian system is chosen in a way that Ox always coincides with the zig-zag direction of the graphene lattice. In these coordinates the tension, \mathbf{T} , reads $\mathbf{T} = T \cos(\theta) \mathbf{e}_x + \sin(\theta) \mathbf{e}_y$. As for any solid, the generalized Hooke’s law relating stress, τ_{ij} and strain ε_{ij} has the form

$$\tau_{ij} = C_{ijkl} \varepsilon_{kl}, \quad \varepsilon_{ij} = S_{ijkl} \tau_{kl} \quad (2)$$

where C_{ijkl} (S_{ijkl}) are the components of the stiffness (compliance) tensor. Since we address only states of planar stress, we resort to the 2-dimensional reduction of the stress and strain tensors. In general the components C_{ijkl} depend on the particular choice of the Cartesian axes. Incidentally, for an hexagonal system under planar stress in the basal plane, the elastic components are independent of the coordinate system. This means that graphene is elastically isotropic [14].

The analysis of strain is straightforward in the principal system $Ox'y'$ where $\mathbf{T} = T \mathbf{e}_{x'}$:

$$\varepsilon'_{ij} = S_{ijkl} \tau'_{kl} = T S_{ijkl} \delta_{kx} \delta_{lx} = T S_{ijxx} \quad (3)$$

Given that only five compliances are independent in graphite (S_{xxyy} , S_{xxxy} , S_{xxxz} , S_{zzzz} , S_{yzyz}) [15], it follows that the only non-zero deformations are

$$\varepsilon'_{xx} = T S_{xxxx}, \quad \varepsilon'_{yy} = T S_{xxyy}, \quad (4)$$

which represent the longitudinal deformation and Poisson’s transverse contraction. If we designate the tensile strain by $\varepsilon = T S_{xxxx}$, the strain tensor can be written in terms of Poisson’s ratio, $\sigma = -S_{xxyy}/S_{xxxx}$

$$\varepsilon' = \varepsilon \begin{pmatrix} 1 & 0 \\ 0 & -\sigma \end{pmatrix}. \quad (5)$$

This form shows that graphene responds as an isotropic elastic medium. We use the value $\sigma = 0.165$ known for graphite [15]. It should be mentioned that when stress is induced in graphene by mechanically acting on the substrate [12], the relevant parameter is in fact the tensile strain, ε , rather than the tension T . For this reason, we treat ε as the tunable parameter. Since the lattice is oriented with respect to the axes Oxy , the stress tensor needs to be rotated to extract information about bond deformations. The strain tensor in the lattice coordinate system reads

$$\varepsilon = \varepsilon \begin{pmatrix} \cos^2 \theta - \sigma \sin^2 \theta & (1 + \sigma) \cos \theta \sin \theta \\ (1 + \sigma) \cos \theta \sin \theta & \sin^2 \theta - \sigma \cos^2 \theta \end{pmatrix}. \quad (6)$$

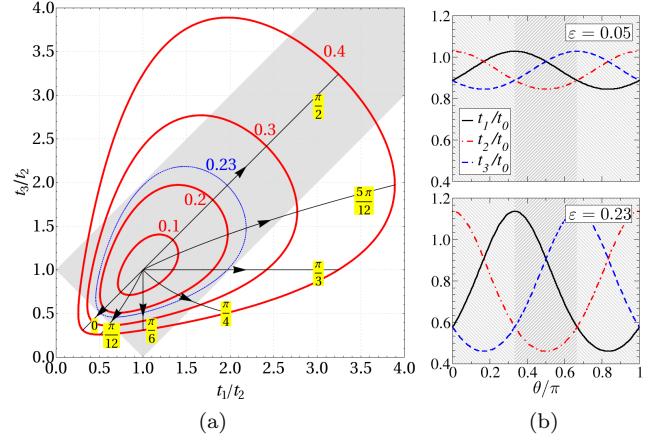


FIG. 2: (Color online) (a) Plot of t_1/t_2 vs t_3/t_2 as a function of strain, ε , and θ . Closed lines are iso-strain curves, and arrowed lines correspond to the trajectory of the point $(t_1/t_2, t_3/t_2)$ as ε increases, calculated at constant angle. The graph is symmetric under reflection on both axes. In the shaded area the spectrum is gapless. The blue iso-strain line ($\varepsilon \approx 0.23$) corresponds to the gap threshold. In panel (b) we show two plots of $t_{1,2,3}$ for $\varepsilon = 0.05$ and $\varepsilon = 0.23$, at $\theta = 0$.

Bond Deformations – Knowing ε_{ij} one readily obtains the deformed bond vectors by means of the transformation $\delta_\alpha = (\mathbf{1} + \varepsilon) \cdot \delta_\alpha^0$. The new bond lengths are given by

$$|\delta_1| \approx 1 + \frac{3}{4}\varepsilon_{11} - \frac{\sqrt{3}}{2}\varepsilon_{12} + \frac{1}{2}\varepsilon_{22} \quad (7a)$$

$$|\delta_2| \approx 1 + \varepsilon_{22} \quad (7b)$$

$$|\delta_3| \approx 1 + \frac{3}{4}\varepsilon_{11} + \frac{\sqrt{3}}{2}\varepsilon_{12} + \frac{1}{4}\varepsilon_{22} \quad (7c)$$

Of particular interest are the cases $\theta = 0$ and $\theta = \pi/2$ since they correspond to tension along the zig-zag (Z) and armchair (A) directions:

$$Z: |\delta_1| = |\delta_3| = 1 + \frac{3}{4}\varepsilon - \frac{1}{4}\varepsilon\sigma, \quad |\delta_2| = 1 - \varepsilon\sigma \quad (8a)$$

$$A: |\delta_1| = |\delta_3| = 1 + \frac{1}{4}\varepsilon - \frac{3}{4}\varepsilon\sigma, \quad |\delta_2|^2 = 1 + \varepsilon \quad (8b)$$

Hopping Renormalization – The change in bond lengths (7) leads to different hopping amplitudes among neighboring sites. In the Slater-Koster scheme [16], the new hoppings can be obtained from the dependence of the integral $V_{pp\pi}$ on the inter-orbital distance. Unfortunately determining such dependence with accuracy is not a trivial matter. Many authors resort to Harrison’s fly-leaf expression which suggests that $V_{pp\pi}(l) \propto 1/l^2$ [17]. However this is questionable, insofar as such dependence is meaningful only in matching the tight-binding and free electron dispersions of simple systems in equilibrium (beyond the equilibrium distance such dependence is unwarranted [17]). It is indeed known that such functional form fails away from the equilibrium distance [18], and a more reasonable assumption is an exponential decay [19]. In

line with this we assume that in graphene

$$V_{pp\pi}(l) = t_0 e^{-3.37(l-a_0)}, \quad (9)$$

where the rate of decay is extracted from the experimental result $dV_{pp\pi}/dl = -6.4 \text{ eV}/\text{\AA}$ [20]. As a consistency check we point out that, according to Eq. (9), the next-nearest neighbor hopping (t') would have the value $V_{pp\pi}(\sqrt{3}a_0) = 0.23 \text{ eV}$, which tallies with existing estimates of t' in graphene [9].

Gap Threshold – The bandstructure of Eq. (1) with arbitrary hoppings t_1, t_2, t_3 is given by

$$E(k_x, k_y) = \pm |t_2 + t_3 e^{-ik \cdot \mathbf{a}_1} + t_1 e^{-ik \cdot \mathbf{a}_2}|. \quad (10)$$

Here both t_α and the primitive vectors \mathbf{a}_α [Fig. 1(b)] change under strain. This dispersion has been previously discussed in Refs. 21, 22. It was found that the gapless spectrum is robust, and that a gap can only appear under anisotropy in excess of 100% in one of the hoppings. More specifically, the spectrum remains gapless as long as the condition

$$\left| \frac{|t_1|}{|t_2|} - 1 \right| \leq \frac{|t_3|}{|t_2|} \leq \left| \frac{|t_1|}{|t_2|} + 1 \right| \quad (11)$$

is in effect. This condition corresponds to the shaded area in Fig. 2(a). Using (6, 7, 9) we have mapped the evolution of the hoppings with ε and θ . This allows us to identify the range of parameters that violate (11), and to obtain the threshold for gap opening. For a given θ , we follow the trajectory of the point $(t_1/t_2, t_3/t_2)$ as strain grows, starting from the isotropic point at $\varepsilon = 0$. The result is one of the arrowed curves in Fig. 2(a). The value of ε at which this curve leaves the shaded area corresponds to the gap threshold for that particular angle. From such procedure, summarized in Fig. 2(a), we conclude that: (i) the gap threshold is at $\varepsilon \approx 0.23$ ($\sim 20\%$); (ii) the behavior of the system is periodic in θ with period $\pi/3$, in accord with the symmetry of the lattice; (iii) tension along the zig-zag direction ($\theta = 0, \pi/3, \dots$) is more effective in overcoming the gap threshold; (iv) tension along the armchair direction never generates a gap.

The two panels of Fig. 2(b) contain polar plots of the individual t_α for two particular deformations. It is clear that, for deformations along the Z direction, the highest relative change occurs along the zig-zag bonds ($t_{1,3}$), and conversely for deformations along the A direction. This could also be anticipated from Eqs. (8) and the smallness of σ .

Critical Gap – The fact that the isotropic point (1, 1) in Fig. 2(a) is surrounded by an appreciable shaded area, means that the gapless situation is robust, and the emergence of the gap requires a critical strain. The physical effect behind such critical gap lies in the fact that, under strain, the Dirac cones drift away from the points \mathbf{K}, \mathbf{K}' in the Brillouin zone (BZ) [9, 23]. This can be clearly seen from inspection of the energy dispersions plotted in

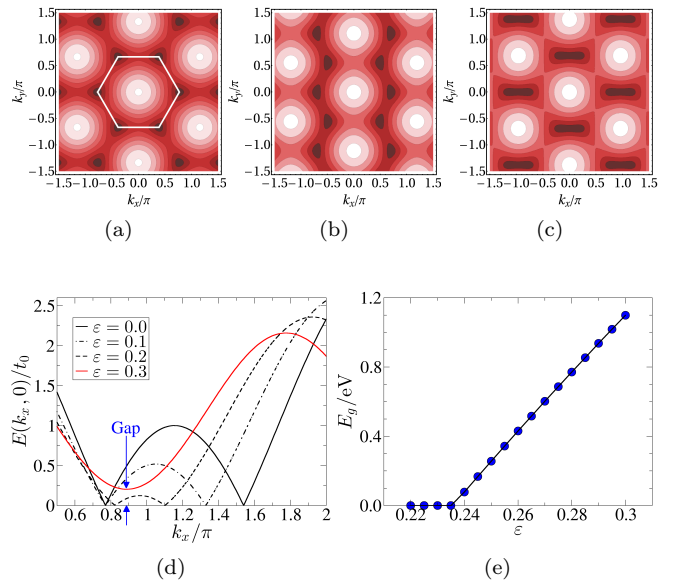


FIG. 3: (Color online) Top row shows density plots of the energy dispersion, $E(k_x, k_y)$, for $\{\varepsilon = 0, \theta = 0\}$ (a), $\{\varepsilon = 0.2, \theta = \pi/2\}$ (b), and $\{\varepsilon = 0.2, \theta = 0\}$ (c). In (d) we have a cut of (c) along $k_y = 0$, showing the merging of the Dirac cones as strain increases, and the ultimate appearance of the gap. In panel (e) we compare the gap given by Eq. (12) (line) with the result obtained from direct minimization of the energy in the full BZ (dots).

Fig. 3(a-c) (the dispersions include the deformation of the BZ). For strain along the A direction the nonequivalent Dirac cones move in opposite directions and never meet [Fig. 3(b)]. However, if the deformation is along the Z direction, the cones always approach each other [Fig. 3(c)], and will eventually merge. This merging is seen in detail in Fig. 3(d) where a cut along $k_y = 0$ is presented. Precisely at the critical point, the dispersion is linear along k_x and quadratic along k_y , which has peculiar implications for the DOS and Landau level quantization [24]. The gap is a result of this Dirac cone merging process, and the origin of the critical strain is now clear: one needs to deform enough to bring the two Dirac points to coincidence. This agrees with the existing understanding that the gapless Dirac spectrum in graphene is robust with respect to small perturbations.

For strain along $\theta = 0$ the gap is conveniently given by

$$E_g(\varepsilon) = 2 |2t_1(\varepsilon) - t_2(\varepsilon)| \theta(t_2 - 2t_1). \quad (12)$$

An example of the strain dependence of E_g can be seen in Fig. 3(e). In it we see the agreement between the gap given by Eq. (12) and the value extracted from a direct minimization of $E(k_x, k_y)$ in the full (deformed) BZ.

From Fig. 3(b) one can see that pulling along an armchair direction imparts 1D-like features to the system: the dispersion becomes highly anisotropic. This is explained on account of the results plotted in Fig. 2(b)

which show that stress along A tends to weaken one bond only. In extreme cases, the weak bond can be highly suppressed leaving only a set of 1D chains [25]. This means that strain along certain directions can be used as a means to induce preferred anisotropy in electric transport. In contrast, pulling along a zig-zag direction tends to dimerize the system, which ultimately explains the appearance of the gap in this case.

Discussion – We see that, within the tight-binding Hamiltonian written in Eq. (1), uniform tension can induce a bulk spectral gap in graphene. However, at least within a non-interacting tight-binding approach, the gap threshold is very difficult to overcome, if at all possible. Since a tensional strain in excess of 20% is required to observe such feature, several comments are in order. We start by noticing that in our calculation we kept only the lowest order terms in ε . In addition, although strain magnitudes of $\sim 20\%$ are not unreasonable, graphene is expected to be in the non-linear elastic regime [3]. Therefore, non-linear corrections can be relevant at the quantitative level in the vicinity of the threshold. Secondly, *ab-initio* calculations seem to show that a gap is present in graphene for arbitrarily small tensions [12, 26]. But is not clear yet whether this is a solid conclusion, or an artifact of DFT. For example there is an order of magnitude discrepancy between the gap predicted in these two references for 1% strain. In addition, Ref. 26 claims their *ab-initio* result agrees with the bandstructure (10) after a suitable choice of hoppings. As we showed above this cannot be the case, since there is always a (large) threshold for the appearance of the gap. Consequently, further clarification regarding *ab-initio* under strain is desired.

It is also possible that the Slater-Koster type Hamiltonian (1) constitutes a severe over-simplification in the presence of strain. The non-orthogonality of the orbitals, the inclusion of further neighbors, or electron-electron interactions could become relevant. For example, Kishigi *et al.* have shown that the inclusion of next-nearest neighbor terms (t') can, alone, engender a gap [27]. But this requires a very specific deformation of the lattice, unlikely to occur under simple tension. The presence of t' can also lead to other effects, like tilted Dirac cones as discussed in Ref. 28. But certainly more likely is the possibility that strained graphene could have different site energies on the A and B sublattices (even for planar strain) which would trivially open a bulk spectral gap.

Whether these issues can be further clarified or not, several effects of tensional strain are clear. If (1) turns out to be a faithful model for graphene under strain — as it is for free graphene —, one could use the gap threshold to monitor/detect high strain states, for mechanical applications. In addition, tension leads to one-dimensionalization of transport in graphene by weakening preferential bonds: transport should certainly be anisotropic, even for small tensions.

Implicit in our discussion so far has been the assump-

tion that our target is exfoliated graphene. Recent investigations show that graphene grown epitaxially on SiC is almost always under strain, imposed by the lattice mismatch and the growth conditions [29]. For these systems, the relaxed starting configuration is already deformed.

Lastly, it is important to point out that, even though a spectral gap seems to require extreme strain, one can generate a *transport* gap by means of local, small, deformations. It has been shown in Refs. [23, 30] that tunneling across a strained region is highly suppressed, and leads to a transport gap (i.e., in the electrical conductivity) at small densities, even in the absence of a bulk spectral gap. We then conclude that strain (local or uniform) can be an effective means of tuning the electronic structure and transport characteristics of graphene devices. Even if the bulk gap turns out to be challenging in practice, local strain could be used as a way to mechanically pinch-off current flow.

We thank enlightening discussions with Y. P. Feng, A. K. Geim, A. Heinz, Y. Lu, Z. Ni, Z. X. Shen, and T. Yu. AHCN acknowledges the partial support of the U.S. Department of Energy under the grant DE-FG02-08ER46512. VMP is supported by FCT via SFRH/BPD/27182/2006 and PTDC/FIS/64404/2006.

-
- [1] M.-F. Yu *et al.*, *Science* **287**, 637 (2000).
 - [2] C. Lee *et al.*, *Science* **321**, 385 (2008).
 - [3] F. Liu, P. Ming, and J. Li, *Phys. Rev. B* **76**, 064120 (2007).
 - [4] A.K.Geim and K. Novoselov, *Nat. Mat.* **6**, 183 (2007).
 - [5] K. S. Novoselov *et al.*, *Science* **306**, 666 (2004).
 - [6] T. Ando and T. Nakanishi, *J. Phys. Soc. Jpn.* **67**, 1704 (1998).
 - [7] K. S. Novoselov *et al.*, *Nature* **438**, 197 (2005).
 - [8] P. R. Wallace, *Phys. Rev. Lett.* **71**, 622 (1949).
 - [9] A. H. Castro Neto *et al.*, arXiv:0709.1163 (2007).
 - [10] M. Y. Han *et al.*, *Phys. Rev. Lett.* **98**, 206805 (2007).
 - [11] L. A. Ponomarenko *et al.*, *Science* **320**, 356 (2008).
 - [12] Z. Ni *et al.*, arXiv:0810.3476 (2008).
 - [13] Z. Ni *et al.*, *ACS Nano* **2**, 1033 (2008).
 - [14] L. D. Landau and E. M. Lifshitz, *Theory of Elasticity* (Pergamon, 1986), 3rd ed.
 - [15] L. Blakslee *et al.*, *J. Appl. Phys.* **41**, 3373 (1970).
 - [16] J. C. Slater and G. F. Koster, *Phys. Rev.* **94**, 1498 (1954).
 - [17] W. A. Harrison, *Elementary Electronic Structure* (World Scientific, 1999), ISBN 981-023895-9.
 - [18] G. Grosso and C. Piermarocchi, *Phys. Rev. B* **51**, 16772 (1995).
 - [19] D. A. Papaconstantopoulos *et al.*, in *Tight-Binding Approach to Computational Materials Science*, edited by P. Turchi, A. Gonis, and L. Colombo (Materials Research Society, Pittsburgh, 1998), p. 221.
 - [20] A. H. Castro Neto and F. Guinea, *Phys. Rev. B* **75**, 045404 (2007).
 - [21] B. Wunsch, F. Guinea, and F. Sols, *New J. Phys.* **10**, 103027 (2008).
 - [22] Y. Hasegawa *et al.*, *Phys. Rev. B* **74**, 033413 (2006).

- [23] V. M. Pereira and A. H. Castro Neto, arXiv:0810.4539 (2008).
- [24] P. Dietl, F. Piechon, and G. Montambaux, Phys. Rev. Lett. **100**, 236405 (2008).
- [25] This is another way to see why strain along A can never lead to a gap.
- [26] G. Gui, J. Li, and J. Zhong, Phys. Rev. B **78**, 075435 (2008).
- [27] K. Kishigi, H. Hanada, and Y. Hasegawa, J. Phys. Soc. Jpn. **77**, 074707 (2008).
- [28] M. O. Goerbig *et al.*, Phys. Rev. B **78**, 045415 (2008).
- [29] N. Ferralis, R. Maboudian, and C. Carraro, Phys. Rev. Lett. **101**, 156801 (2008).
- [30] M. M. Fogler, F. Guinea, and M. I. Katsnelson, arXiv:0807.3165 (2008).